

Repair of soda–lime–silica glass

Kyriaki Corinna Datsiou · Dominic Hall ·
Mauro Overend

Received: 16 January 2018 / Accepted: 28 March 2018 / Published online: 5 April 2018
© The Author(s) 2018

Abstract Glass strength is very sensitive to damage accumulation during its service life. Repair methods for glass have been proposed over the last decades to volumetrically fill or remove existing flaws from the surface of glass. However, the lack of information on the strength recovery attributable to glass repair methods restrict their use to low consequence class applications in buildings thereby making replacement of damaged installed glass the only safe and practical solution when dealing with damaged glass. Repair methods involving volumetric filling of visible flaws with resins, removal of visible flaws with polishing and chemical repair with acid treatment of visible flaws are undertaken in this study to investigate the strength recovery in 60 artificially aged annealed glass specimens. It is found that the polishing provides the most promising strength recovery results showing a 132 and a 40% increase in design and mean strength whilst the acid treatment provides the worst performance. Polishing repairs are further investigated in this study to determine their efficacy in strength recovery after environ-

mental ageing (exposure to UV, humidity and freeze-thaw cycles).

Keywords Glass · Repair · Strength recovery · Resin repair · Polishing · Acid repair · Environmental ageing of repair

1 Introduction

Glass is an ubiquitous material, 87% of glass [52 million metric tonnes per annum (Nsg 2010)] is used in sheet form and is used extensively in vision and display panels in the automotive, aerospace and construction industry. Glass has many desirable properties, but it is very sensitive to damage accumulation; flaws (Fig. 1a) accumulate on the surface of glass during its service life and have a detrimental effect on its strength because: (a) they generate stress concentrations at the flaw tip that are several orders of magnitude higher than the nominal stress in the immediate vicinity of the flaw and; (b) they impose this stress concentration at a flaw depth α below the surface thereby reducing or removing the beneficial effect of residual surface compression induced by glass toughening processes (Fig. 1b).

Previous research showed an 85% reduction in design strength in naturally aged annealed glass exposed for 20 years to erosive action (Datsiou and Overend 2017a, b). Similarly, a reduction in design strength of 19 and 98% was found respectively in fully toughened and chemically toughened glass when exposed to equiva-

Electronic supplementary material The online version of this article (<https://doi.org/10.1007/s40940-018-0064-y>) contains supplementary material, which is available to authorized users.

K. C. Datsiou (✉) · D. Hall · M. Overend
Glass and Façade Technology Research Group,
Department of Engineering, University of Cambridge,
Cambridge CB2 1PZ, UK
e-mail: kdatsiou@gmail.com

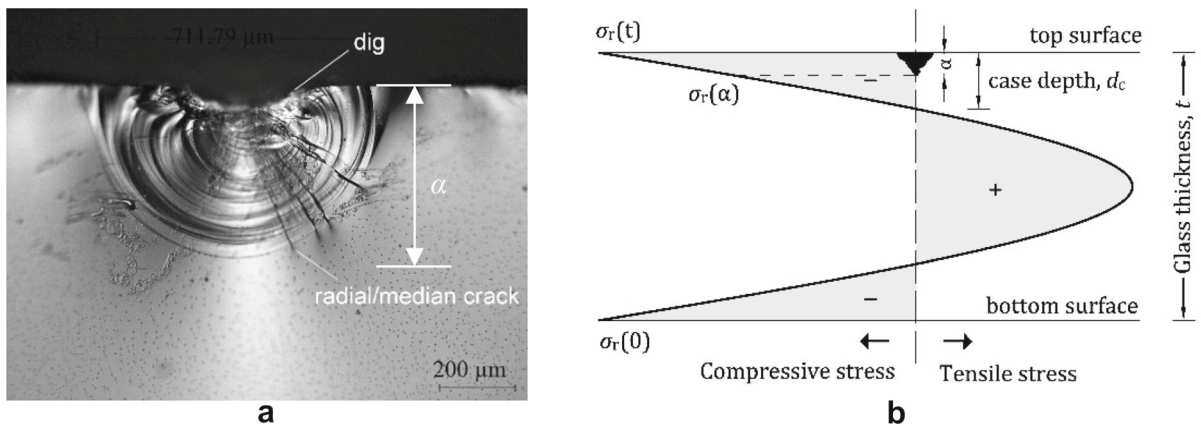


Fig. 1 Cross section of critical flaw in: **a** annealed glass (micrograph) and; **b** stress profile of fully toughened glass

lent artificial ageing (Datsiou and Overend 2017a, b). Repair methods have been proposed over the past years to partly recover the strength of damaged glass; these are volumetric filling, removal, chemical treatment or thermal treatment of surface flaws in damaged glass.

Resin repair is the most widespread, commercial glass repair option and mostly targets damaged vision panels in automotive applications. This method involves the injection of a clear, acrylic or epoxy resin under pressure to volumetrically fill visible surface flaws. Previous research showed a varying strength recovery in resin repaired glass; acrylic resins were found to be superior to epoxy resins (Overend and Louter 2015), however, epoxy resins were found to produce a larger improvement in strength in repaired glass in (Hand et al. 2003). This difference could be potentially attributed to differences in accounting for the influence of subcritical crack growth during the destructive tests in the two studies. Additionally, poly-ether-ketone resins have excellent mechanical properties and could potentially be used for glass repair, but the processing temperature to achieve transparency needs to be above 300 °C and are therefore, impractical for in-situ glass repairs. The same applies to sol-gels as they generally require a high-temperature firing process. The physical mechanism behind the strength recovery is mainly attributed to the suppression of sub-critical crack growth phenomena as water diffusion at the crack tip is prevented after repair (Overend and Louter 2015). However, the durability of resins or their efficiency to penetrate to the deepest parts of the flaws and prevent water diffusion are not well documented.

Alternative repair methods include polishing of the damaged glass; material is gradually removed from the glass surface by abrasion until all visually discernible parts of the flaw are removed. The physical mechanism behind this is that cracks would no longer act as stress concentration points. This method is again common practice for glass in automotive applications, with companies selling polishing kits claiming strength improvements in the region of 35% (Glass Polish Ltd 2017). Polishing of glass with sanding pads can however, lead to the introduction of additional flaws on the glass surface (Hayashida et al. 1972; Schula 2015).

Chemical treatment has been also identified as a potential method for strength recovery in damaged glass. Sufficient exposure to hydrofluoric acid can lead to an increase in glass strength as pre-existing surface flaws become blunt; however, the increase in strength is accompanied with loss of transparency and decrease in optical transmission depending on the concentration of the hydrofluoric acid (Dabbs and Lawn 1982; Kolli et al. 2009). Alkali leaching at the crack tip in the presence of water, were found to change the chemical composition of the glass and to increase its strength (Gehrke et al. 1991). In particular, strength increase was promoted in acidic environments. Additionally, thermal treatment by heating of the glass component up to its transition temperature, followed by subsequent annealing, resulted in an up to 35% increase in strength (Zaccaria and Overend 2015). However, this method is impractical for in-situ glass.

Given the limited evidence-based research and the lack of understanding on the strength recovery and the ageing of repairs, it is unsurprising that the preferred



Fig. 2 Examples of glass panels with increased size, complexity and cost in architectural applications: **a** Apple Zorlu Centre in Istanbul (© www.fosterandpartners.com) and; **b** Apple Store at 5th Avenue – New York (© www.ecengineers.com)

approach, when dealing with high consequence of failure glass components that have been damaged in transit or during their service life, is to replace the glass component altogether. This remains a sensible and viable approach for small, low cost, and easy-to-replace glass panels, but as the size, complexity and cost of glass panels continues to increase (Fig. 2a, b), the replacement and disposal of the damaged glass becomes costly and unsustainable.

This paper investigates the effectiveness of 3 different types of repair methods on damaged glass. These involve: (a) resin repair using two commercially-available resins: an acrylic and a methacrylate resin; (b) flaw removal with polishing of the glass surface using a hand-held rotary power tool with fitted sanding pads and; (c) chemical repair using a solution of hydrochloric acid to achieve an acidic and humid environment at the flaw tip. These methods are implemented on carefully pre-damaged annealed glass specimens that are artificially aged in a controlled dropped gravel set-up. The best performing repair method is subsequently environmentally aged to assess its performance after ageing. The main aim of the paper is to quantify the aesthetic appearance and the strength recovery of each repair method compared to unrepaired and as-received glass. Section 2 below provides an overview of the specimens and describes the experimental methods used for the ageing, the repair and the destructive tests in this study. Section 3 presents the salient results and observations for each repair method. Finally, salient conclusions are summarized in Sect. 4.

2 Specimens and methods

135 soda lime silica annealed glass specimens were cut from sheet stock and used for the purpose of this study. These specimens were grouped in 9 series of 15 specimens (Table 1). One series was the control series and was tested destructively in its as-received form (AR) whilst the remaining 8 were artificially aged in a controlled manner to introduce two flaws on the tin surface of each glass specimen. The first (AA) of the artificially aged series was tested destructively after ageing without any post-processing whilst the remaining 7 were repaired as follows:

- 2 series were resin injected (RR1: acrylic resin and RR2: methacrylate resin);
- 4 series were polished: one (PR) was tested destructively after repair and the rest were exposed to environmental ageing after repair, namely, immersion to water (PR-W), freeze-thaw cycles (PR-FTC) and UV irradiation (PR-UV) and;
- 1 series was treated with hydrochloric acid (ATR).

Below follows a description of the experimental procedure used in this study.

2.1 Artificial ageing

The sand trickling rig in (Datsiou and Overend 2017a, b) was used to artificially induce controlled flaws in series AA, RR1, RR2, PR, PR-W, PR-FTC, PR-UV and ATR. Each specimen was clamped on a stationary platform, titled at 45° to the floor. Two rounded riverside gravel weighing approximately 10 g each, were allowed to

Table 1 Series overview

Series	Glass type	Processing	Specimens	Dimensions (mm)
AR	Annealed SLS glass	As-received	15	150 × 150 × 3
AA	Annealed SLS glass	Artificially aged	15	150 × 150 × 3
RR1	Annealed SLS glass	Acrylic resin repair #1	15	150 × 150 × 3
RR2	Annealed SLS glass	Acrylic resin repair #2	15	150 × 150 × 3
PR	Annealed SLS glass	Polishing repair	15	150 × 150 × 3
ATR	Annealed SLS glass	Acid treatment repair	15	150 × 150 × 3
PR-W	Annealed SLS glass	Repaired—exposure to water	15	150 × 150 × 3
PR-FTC	Annealed SLS glass	Repaired—exposure to freeze thaw cycles	15	150 × 150 × 3
PR-UV	Annealed SLS glass	Repaired—exposure to UV	15	150 × 150 × 3

fall freely through a 3 m long guide tube on the tin surface of each glass specimen. Heavier gravel were not considered as they triggered fracture in the glass during impact. Additionally, a second drop of 10 g gravel resulted in fracture of the glass specimen and therefore the selected level of damage was close to the maximum damage the glass could sustain without fracture for the given drop height. Moreover and based on the recommendations of ASTM C1036-16 (2011), the induced damage would lead to rejection of the glass during quality control processes.

After the artificial ageing, the samples were stored in ambient laboratory conditions ($T \approx 20^\circ\text{C}$ and $RH \approx 50\%$) for one week before being repaired.

2.2 Repair

The following three repair scenarios were investigated: resin repair (RR); polishing (PR) and acid treatment (ATR).

2.2.1 Resin repair

Two commercial acrylic resins that are commonly applied for repairing damaged glass in the automotive industry, were used in this study. The first (RR1) was primarily of acrylic composition (1-vinyl-2-pyrrolidone and isobornyl acrylate) while the second (RR2) of methacrylate composition (primarily benzyl methacrylate, 2-hydroxyethyl methacrylate, isobornyl acrylate, octyl acrylate and decyl acrylate). Both resins claim to conform to BS-AU 251 (1994), on the repair of automotive laminated glass windscreens.

The repair (Fig. 3) comprised the following steps following the directions of the supplier:

- The injector barrel is positioned over the flaw and pressed manually to ensure a good seal;
- Resin is injected with a syringe in the barrel (Fig. 3a);
- The syringe is withdrawn and a piston is screwed into the barrel to increase the pressure and force the resin into the flaw; the barrel remains under pressure for a duration of 3 min (Fig. 3b);
- The piston is subsequently un-screwed slightly (≈ 10 mm) to induce suction and remove any residual air for a duration of 30 s;
- The same progress cycle is then repeated for a second time i.e. the injector is pressurized for 3 min and subsequently suction is induced for 30 s;
- The injector is then removed and any excess resin is gently wiped away;
- The repaired area is cured under a UV light for a duration of 5 min.

2.2.2 Polishing

A combination of coarse and fine sanding pads were used for polishing repair. These were fitted to a Dremel rotary power tool, which rotated at a speed of 5000 rpm. The method involves the following steps:

- The coarsest sanding pad (GP 100) is used to remove any visible parts of the flaw from the glass surface. The rotary is moved in two orthogonal directions across the flaw stopping at different locations at the end of each motion to avoid the formation of a step on the glass surface. The repaired area

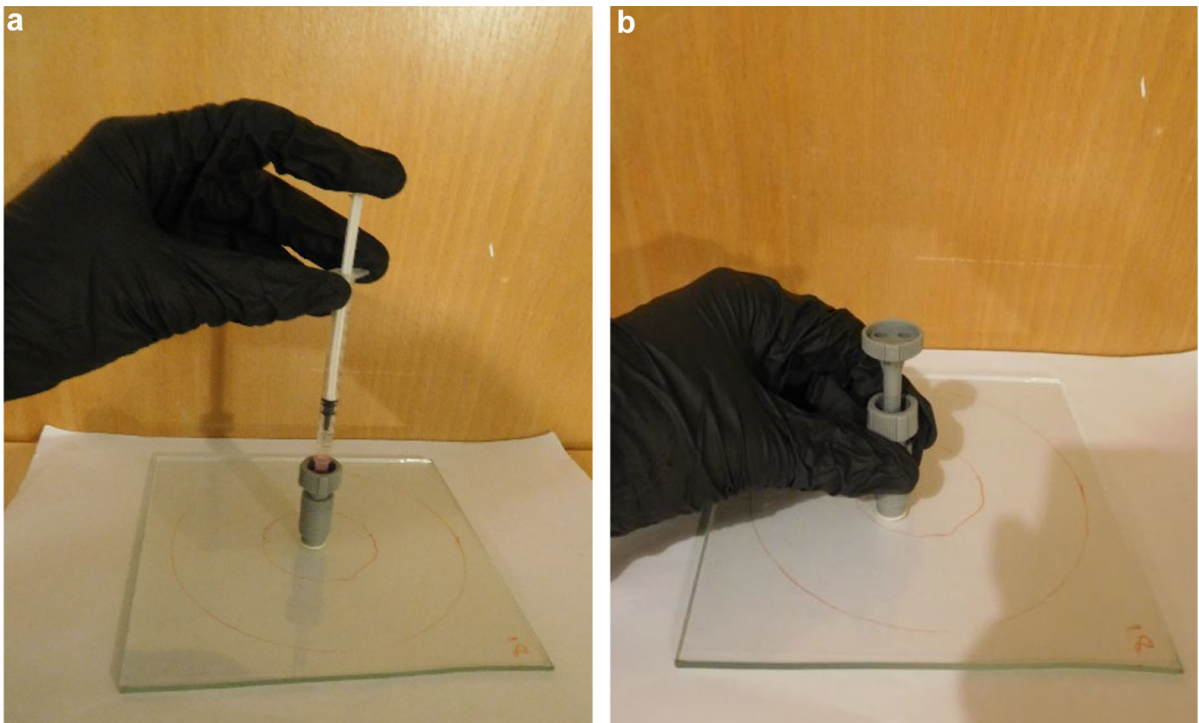


Fig. 3 Resin repair **a** resin injection and; **b** application of pressure to force the resin into the flaw



Fig. 4 Polishing repair: glass surface after polishing with: **a** coarse sanding pad; **b** fine sanding pad and; **c** rayon felt polishing pad

acquires an even, cloudy white surface at the end of this step (Fig. 4a);

- The finer sanding pad (GP 50) is then fitted and the rotary is again moved across the flaw in a similar manner until the repaired area acquires an even, light haze, with no dark marks or abrasion scratches (Fig. 4b) and;
- A rayon felt polishing pad is subsequently fitted to the rotary and a small amount of cerium oxide polishing compound (suspension of CeO_2 particles

with an average diameter of $1.2 \mu\text{m}$) is applied to the repaired area. The rotary and compound are moved slowly across the repaired area to polish it to a clear, glossy finish (Fig. 4c) and complete the repair process. As the compound dries out, a small amount of water is sprayed onto the glass to reactivate the compound. The glass surface is then wiped clean to remove any residual polishing compound.

Throughout this process, the glass surface is periodically checked to ensure the temperature does not

increase. If the surface feels warm to the touch, a small amount of water is sprayed from a handheld vaporiser to cool it.

2.2.3 Acid treatment

The acid treatment repair was based on the observations of Gehrke et al. (1991) that alkali leaching in the presence of water at the crack tip could lead to strength increase which is promoted in acid environments. A solution of hydrochloric acid was applied to the flaw in an attempt to change the crack tip composition. Glass is chemically resistant to hydrochloric acid and also surface abrasion or changes in flaw morphology are not expected, therefore any strength recovery will be due to the changes in the chemical composition at the crack tip. The procedure is outlined as follows:

- A drop (0.05 ml) of 0.1 molar hydrochloric acid solution is released on the flaw with a pipette and left for 60 min;
- The acid is then carefully wiped off the glass surface and;
- The glass is cleaned with a small amount of water and allowed to dry.

2.3 Ageing of repairs

The performance after environmental ageing of the repair method that provided the highest strength recovery is investigated in Sect. 3.3 of this study. Three ageing scenarios were used: (a) immersion in water, (b) freeze-thaw cycles and; (c) ultraviolet light irradiation. The environmental ageing of the repaired glass performed in this study is not correlated to the service life of the glass, but is a preliminary investigation of the effects of UV light, freeze thaw cycles and water immersion on repaired glass. This is expected to form the basis for a more detailed investigation in future work where realistic environmental ageing scenarios will be considered. Further details on each environmental ageing scenario follow below.

2.3.1 Water immersion

Exposure to water involved submerging a series of 15 repaired glass (PR-W) specimens in a container of distilled water for 4 days. Distilled water was selected to

prevent the influence of any dissolved impurities on glass strength degradation / recovery. The series was subsequently dried in an oven at 60 °C for 4 h and was then allowed to cool slowly to ambient temperature for 1 h before the destructive tests.

2.3.2 Freeze-thaw cycles

A series of 15 repaired specimens (PR-FTC) was exposed to freeze-thaw cycles for approximately 4 days. The specimens were placed in a custom-made environmental chamber (Paparo and Overend 2017) with temperatures cycling between -6 and $+26$ °C every 5 h for 19 cycles. The specimens were subsequently dried in an oven at 60 °C for 1 h, to remove humidity arising from any condensation inside the chamber, and were then allowed to slowly cool to ambient temperature for 1 h before the destructive tests.

2.3.3 UV exposure

A series of 15 repaired specimens (PR-UV) was exposed to ultraviolet irradiation for 2 days with a 300W Osram Vitalux bulb. The series was irradiated in two batches of 7 and 8 specimens to ensure an even irradiation across all samples. The bulb was mounted at a distance of 45 cm above the samples, to provide a balance between maximising the strength of irradiation and reducing excessive heating on the glass surface achieving a 19.6 times stronger UV irradiation at the glass surface when compared to sunlight [$UV_{exp} = 78.3 \text{ W/m}^2$ vs. $UV_{sun} = 4 \text{ W/m}^2$, calculations based on ASTM G173-03 (2012) and MacKay (2009)].

2.4 Destructive testing and strength analysis

A Coaxial Double Ring set-up conforming to ASTM C1499-03 (2009), with a 51 and 127 mm diameter respectively for the loading and the reaction ring, was used for the destructive tests of the glass specimens. A stress rate of 20 MPa/s was selected to minimize the influence of sub-critical crack growth (Datsiou 2017). The failure load was transformed into failure stress based on the numerical model developed in (Datsiou and Overend 2017a, b) for the Coaxial Double Ring set-up and the specific dimensions of the annealed glass specimens used in this study. The stress data were then

converted to an equivalent strength of 60 s (Eq. 1) and fitted to a 2-parameter Weibull distribution (Eq. 2) with a weighted least square regression method using Hazen’s estimator and Faucher and Tyson’s weight function (Datsiou and Overend 2018). This follows the findings of Datsiou and Overend (2018) who showed that this approach provides a better fit than other distributions (e.g. normal and the lognormal) and other popular parameter estimating methods.

$$\int_0^{t_f} \left(\frac{\sigma_f \cdot t}{t_f}\right)^n dt = \int_0^{t_{ref}} \sigma_{f,60}^n dt$$

$$\Rightarrow \sigma_{f,60} = \sigma_f \cdot \left[\frac{t_f}{t_{ref} \cdot (n + 1)}\right]^{1/n} \tag{1}$$

where σ_f : the failure stress and n : the exponential crack velocity parameter also known as static fatigue constant ($n = 16$ for laboratory conditions used in this study (Haldimann et al. 2008)).

$$P_f(\sigma_{f,60}) = 1 - \exp\left[-\left(\frac{\sigma_{f,60}}{\theta}\right)^\beta\right] \tag{2}$$

where P_f : the probability of failure, β : the shape factor and θ : the scale factor of the Weibull distribution.

3 Results

The statistical analysis of the strength data is presented below; cumulative function plots of the Weibull distribution are provided in Sects. 3.1–3.3 for all series while

salient fractile, extreme and goodness of fit values are reported for each series in Table 2. The salient fractile values correspond to the mean strength (probability of failure $P_f = 0.5$) and the design strength (probability of failure $P_f = 0.008$) following the recommendations of ASTM 1300-09).

3.1 Fracture strength of as received and artificially aged series

Artificial ageing consisted of 2 gravel impacts resulting on 2 separate flaws on the glass surface of each specimen e.g. Fig. 5a, b. In all of the artificially aged specimens, the fracture was found to originate from the location of one of the induced flaws. The cumulative distribution functions (CDFs) in Fig. 6a show that the artificially aged (AA) glass is significantly weaker than the as-received (AR) glass; a 68 and 65% reduction in strength is observed for the design ($P_f = 0.008$) and the mean ($P_f = 0.5$) strength respectively. The analogous reduction in strength for both fractile values is attributed to similar values of shape factor, β , of the Weibull distribution ($\beta_{AR} = 5.2$ and $\beta_{AA} = 4.8$, Table 2), which define the slope of the CDFs. Naturally aged glass typically exhibits low values of shape factor, which are of the same order of magnitude as those of the AA glass (Datsiou and Overend 2017a, b), thereby indicating that the artificial ageing method selected in this study is close to reality.

Table 2 Destructive tests and statistical analysis results

Series	Weibull parameters			Extreme values		Fractile values	
	Shape factor β	Scale factor θ	Goodness of fit p_{AD}	Min stress σ_{min} [MPa]	Max stress σ_{max} (MPa)	Design strength $\sigma_{0.008}$ (MPa)	Mean strength $\sigma_{0.50}$ (MPa)
AR	5.22	94.87	0.26	41.87	131.47	37.63	88.44
AA	4.77	33.28	0.22	16.33	45.92	12.10	30.82
RR1	6.29	42.14	0.50	28.61	49.60	19.58	39.76
RR2	9.32	37.89	0.07	28.88	46.40	22.58	36.43
PR	10.38	44.58	0.71	35.94	48.83	28.01	43.04
ATR	5.60	40.32	0.33	27.42	50.24	17.03	37.77
PR-W	5.61	55.68	0.54	37.84	65.44	23.57	52.16
PR-FTC	4.16	49.70	0.06	33.54	66.12	15.59	45.51
PR-UV	4.75	46.72	0.30	32.54	61.39	16.91	43.24

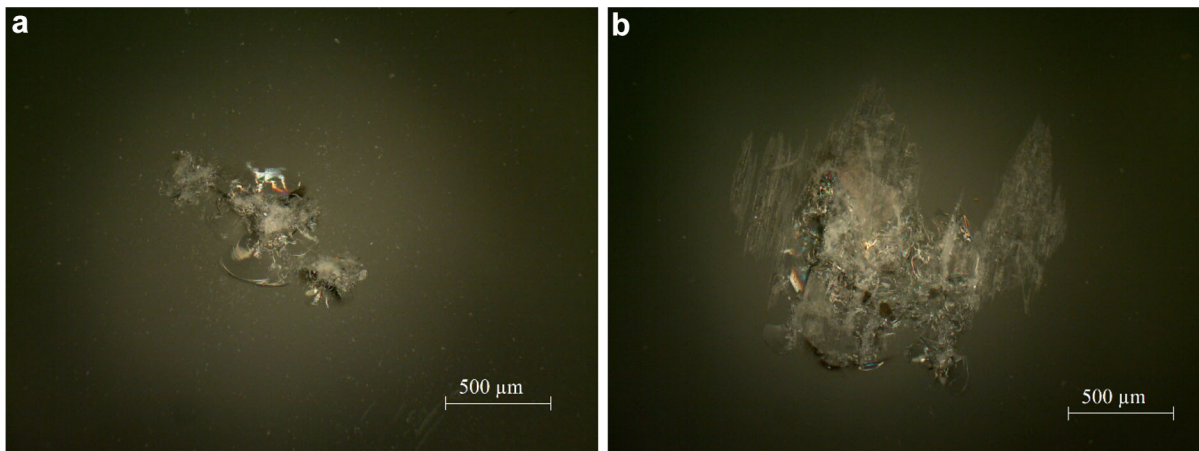


Fig. 5 a, b Artificial ageing: gravel impact flaws in AA glass

3.2 Fracture strength of repaired series

3.2.1 Resin repair

Both methods of resin repair (RR1 and RR2) increased the strength of the artificially aged (AA) glass (Fig. 6b); the highest strength recovery occurs at the low probabilities of failure with the design strength showing a 62 and 87% increase for the acrylic resin (RR1) and the methacrylate resin (RR2) respectively while a 29 and 18% increase is found for the mean strength for RR1 and RR2 respectively (Table 2). This increase in mean strength is similar to the 33 and the 30% increase found in Overend and Louter (2015) for acrylic resin repairs in scratched and intended glass specimens. Similarly to what is reported in Overend and Louter (2015), neither of the resins restores the strength of repaired glass to its as-received (AR) state; the shortage in strength compared to the AR glass was 48 and 55% for RR1 and 40 and 59% for RR2 at design and mean probabilities of failure, respectively. The increase in strength is potentially attributed to the restriction of sub-critical crack growth at the crack tip as water ingress is prevented by the resin. However, the value of the static fatigue parameter was kept constant ($n=16$) during the data analysis stage as this was not validated experimentally.

The methacrylate resin (RR2) resulted in a significantly higher shape factor than AA leading to a steeper CDF (Fig. 6b). This suggests that the efficacy of Resin #2 in strength recovery depends on the flaw size; it has a larger influence on the more severe flaws i.e. the flaws located on the lower end of the CDF. In contrast, the

shape factor of the acrylic resin (RR1) is closer to that of the artificially aged glass (Table 2) and therefore, the efficacy of Resin #1 is more uniform across all flaw sizes.

Visually, some improvement was observed in all resin repaired glass specimens, irrespective of the composition of the resin; the flaws became less prominent, however, parts of the flaws remained visible when viewed at a closer distance or with a magnifying lens.

3.2.2 Polishing repair

Polishing repair (PR) produced a significant improvement in strength for both mean and design probabilities of failure (Fig. 6c) when compared to the artificially aged series (AA); a strength increase of 132 and 40% were noted for $P_f = 0.008$ and $P_f = 0.50$ respectively. However, the strength of the polish-repaired glass was inferior to that of as-received glass (AR) with a 25 and 51% shortfall in strength compared to its as-received state (Table 2).

Similarly to RR1, the shape factor of the CDF also increased considerably compared to that of AA glass leading to a steeper CDF (Fig. 6c). This indicates that the efficacy of the polishing repair is not the same for each flaw and could be potentially attributed to the occurrence of radial flaws in some artificially aged glass specimens. In other words, polish repair could be efficient in removing large visible pits on the glass surface but parts of median cracks or deep radial cracks, indiscernible to the naked eye, could remain in the glass mass after repair, thus decreasing the efficacy of the

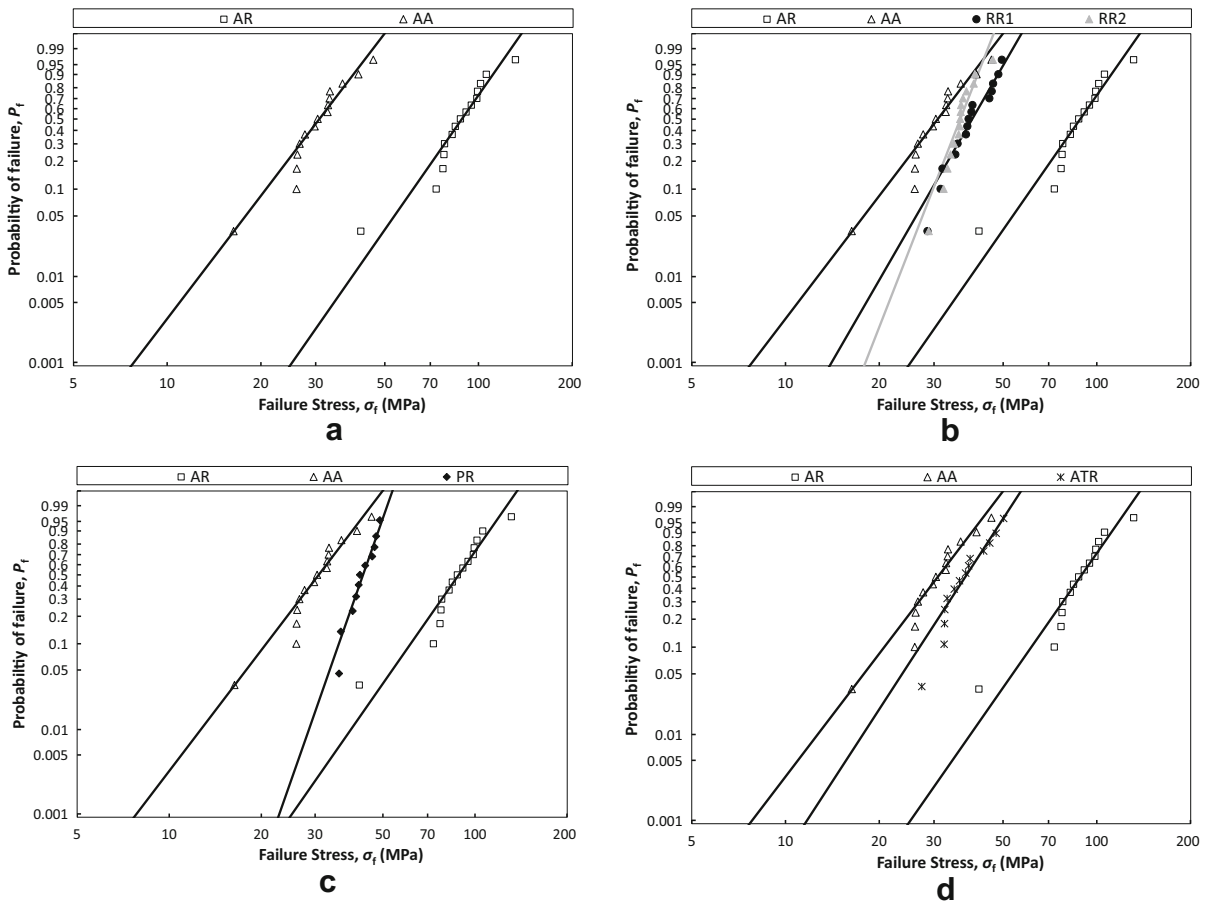


Fig. 6 CDF plots for: **a** as-received (AR) and artificially aged (AA) glass; **b** Resin repair #1 (RR1) & #2 (RR2); **c** polishing repair (PR) and; **d** acid treatment repair (ATR)

repair. Experimental fractographic evidence supports this hypothesis as it reveals that most, but not all, of the critical flaws of the AA series were accompanied by radial cracks (Fig. 7a, b). Another possible scenario behind the increased shape factor is that polishing repair may have fully removed the artificially induced flaws but introduced some additional, but less critical, flaws during the process via the sanding pads (Schula 2015); these flaws would be of homogeneous nature in all specimens leading thus to a steep CDF.

Polishing reduced the thickness of the glass by several tens of microns. Even though this reduction might not be important for annealed glass (approx. 1–3%), it could be detrimental for chemically toughened glass whose case depth of residual surface compression is the order of tens of microns. Therefore, alternative methods would need to be found for the repair of chemically

toughened glass whilst for heat strengthened and / or fully toughened glass, polish repair needs to be evaluated on a case-by-case basis since the case depth is, in this case, a function of the glass thickness.

The polish repair resulted in an aesthetically pleasing appearance; the flaws were no longer visible to the naked eye (Fig. 4c). At very shallow viewing angles, some out-of-flatness could be observed due to material removable. With refinement and better control of the polishing process, it is expected that an even more gradual thickness change could be achieved that would be indiscernible to the naked eye.

3.2.3 Acid treatment repair

Acid treatment repair (ATR) resulted in strength recovery with a 41 and a 23% strength increase for the design

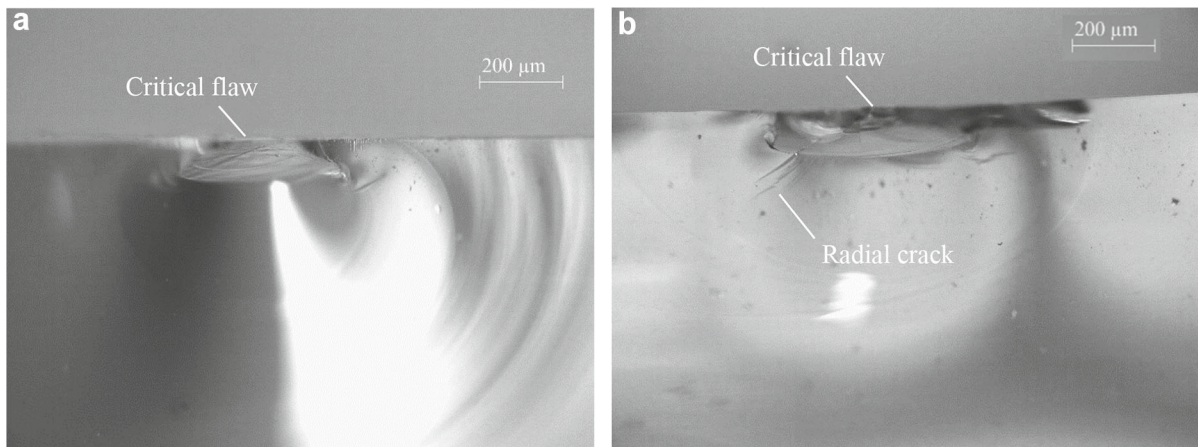


Fig. 7 Critical flaws in AA glass: **a** without radial cracks and; **b** with radial cracks

and the mean probabilities of failure compared to the unrepaired artificially aged series (AA). This supports the findings of Gehrke et al. (1991) that the presence of water and acidic environments could lead in strength increase. Additionally, the ATR series was found to be 55 and 57% short of strength compared to the as-received (AR) series for design and mean probabilities of failure.

The shape factor of the Weibull distribution remained very close to that of the AA series; this potentially denotes that the hydrochloric acid solution had a similar effect on all flaws and therefore, the flaw size or the occurrence of radial cracks is not important in this case.

Visually, there was no noticeable change in the appearance of the repaired flaws.

3.2.4 Comparison of repair methods

All repair methods resulted in increased strength when compared to the unrepaired series (AA). In particular, the highest strength recovery at design level ($P_f = 0.008$) was found for the polishing repair method (PR), followed by the methacrylate resin repair (RR2), the acrylic resin repair (RR2) and lastly the hydrochloric acid treatment (ATR). Polishing (PR) also provided the highest strength increase for the mean probabilities of failure, followed by the acrylic resin repair RR1, the hydrochloric acid treatment (ATR) and lastly the methacrylate resin repair (RR2). However, none of the repair methods was able to achieve a complete strength recovery and reach the as-received strength of glass (AR).

Polishing is therefore, superior to the rest of the repair methods in this study both in terms of strength increase and also visual appearance. The environmental ageing of the repaired glass is investigated only for the most promising method i.e. polishing, in the following section of this study.

3.3 Fracture strength of environmentally aged repaired series

Three series of glass were exposed to different environmental scenarios (immersion in water, freeze-thaw cycles and UV irradiation) for 4 days after being repaired with polishing.

3.3.1 Water immersion

Polish-repaired glass specimens exhibited a wider range of fracture strengths after immersion in distilled water for 4 days (PR-W, Table 2); the strength ranged between $38 \leq \sigma_f \leq 65$ MPa for PR-W whilst the strength of non-aged polished glass (PR) ranged between $36 \leq \sigma_f \leq 49$ MPa.

The increase in strength could be potentially attributed to alkali leaching at the crack tip leading to changes in the chemical composition of the glass after exposure to water (Gehrke et al. 1991). This outcome is also in agreement with (Datsiou and Overend 2017a, b) where a similar increase in strength was noticed after exposure to water for 7 days. The larger scatter in strength data for PR-W led to a reduced shape factor and therefore,

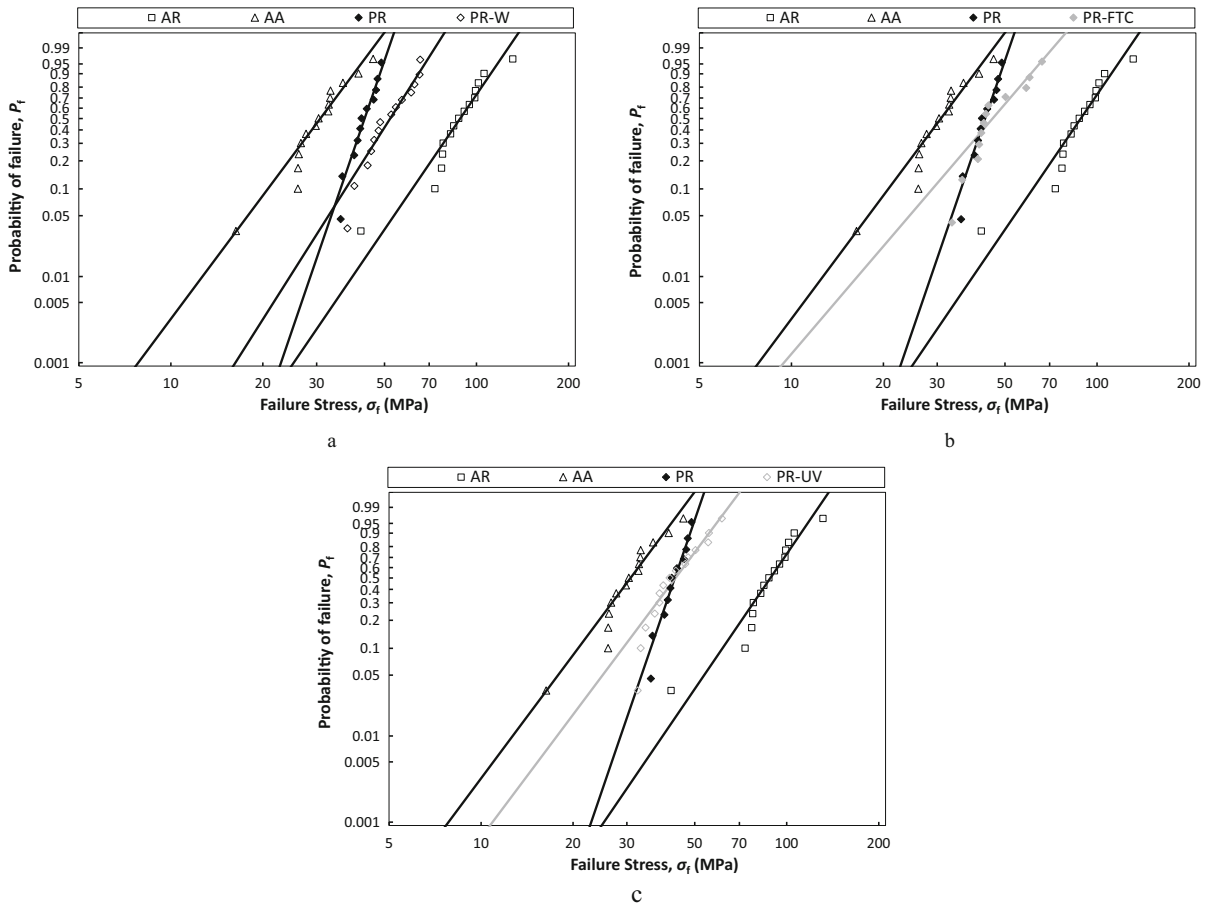


Fig. 8 CDF plots for polish repaired glass (PR) and environmentally aged polish repaired glass after exposure to: **a** water (PR-W); **b** freeze-thaw cycles (PR-FTC) and; **c** UV irradiation (PR-UV)

a shallower slope and a corresponding rotation of the CDF (Fig. 8a). A reduction of 15% is found for this reason for the design strength whilst an increase of 21% is found for mean strength.

3.3.2 Freeze-thaw cycles

Freeze-thaw ageing of the polish-repaired glass specimens involved repeated temperature cycles ranging from -6 to 26°C every 5 h. Most of the specimens that underwent freeze-thaw cycles (PR-FRC) exhibited very similar fracture strengths as the unaged, polish-repaired series (PR) with their fracture strength data coinciding in the CDF plots (Fig. 8b). This was true for all except the last 3 specimens at the upper end of the CDF of the PR-FTC series that showed increased strength. This strength increase could be ran-

dom (i.e. more efficient repair during polishing) or again attributed to alkali leaching at the crack tip as a result of the condensation inside the environmental chamber. Further testing is required to establish the root cause of this strength increase.

The design strength of the PR-FTC is found to be 44% smaller than the strength of the PR series while the mean strength is 6% higher. However, the low goodness-of-fit of the Weibull distribution for the PR-FTC series ($p_{AD} = 0.06$, Table 2) suggest that these percentages should be treated with caution.

3.3.3 UV irradiation

Exposure of the polish-repaired glass specimens to UV irradiation for 4 days (PR-UV) resulted in a larger scatter in strength data when compared to non-aged PR

series (Table 2). This larger scatter led to a smaller shape factor and therefore, a shallower slope and a corresponding rotation of the CDF (Fig. 8c) similar to the PR-W series. The mean strength remained largely unchanged before and after exposure to UV; however, the design strength showed a 40% reduction after UV irradiation as a result of the rotation of the CDF. The physical mechanisms behind this strength decrease are unknown and require further investigations in a future study.

4 Conclusions

This study investigated 3 repair methods namely acrylic and methacrylate resins, polishing and hydrochloric acid treatment for gravel impact flaws in glass. All repair methods resulted in strength increase but their efficiency differed. Polishing was found to be superior to the other repair method in terms of strength recovery but also its aesthetic appearance of the repaired glass whilst acid treatment had the worst performance. A strength improvement of 132 and 40% was found respectively at design and mean probabilities of failure after polish-repair. However and despite its superior performance, polishing was unable to achieve full strength recovery and failed to reach the strength of as-received glass by 25 and 51% respectively at design and mean probabilities of failure. This is attributed to the removal of the visible parts of the flaws, potentially neglecting deeper radial cracks that could not be discerned with naked eye inspection during polishing.

Environmental ageing (water immersion, freeze-thaw cycles and UV irradiation) of polish-repaired glass produced unexpected fracture strength results; strength was increased at mean probabilities of failure whilst strength decreased at design probabilities of failure. This was evidenced by a significant rotation of the Weibull distribution due to the larger scatter of the obtained strength data compared to the non-aged, polish-repaired glass. This larger scatter was caused by a strength increase at the higher fractiles (i.e. smaller flaws). This could be attributed to a phenomenon also suggested by other researchers: alkali leaching at the crack tip in the presence of water. The water is present in the water immersion series and as condensation in the freeze-thaw cycle series. However the similar strengthening effect on exposure to UV has not been reported before and merits further investigation. From the data

in the present study it appears that, environmental ageing, does not have a significant deleterious effect on polish-repaired glass, but further investigation, involving longer durations of ageing and a larger number of specimens, are needed to understand the physical mechanisms behind these observations. Furthermore, synergistic effects should be investigated by combining the ageing tests and accelerated outdoor testing so that they are more representative of real operating environments and account for secondary influences such as airborne pollutants and biological factors.

Further investigation is also necessary to devise a repair method that could achieve full strength recovery for damaged glass. Surface material removal was identified as the best performing method for annealed glass and therefore, this study provides useful insights e.g. to further refine this method to target radial cracks through polishing or other material removal methods e.g. hydrofluoric acid. Despite its poor performance in this study, resin repair could have a role in the repair of chemically toughened glass where material removal would be inadvisable due to the small case depth of residual surface compression.

Open Access This article is distributed under the terms of the Creative Commons Attribution 4.0 International License (<http://creativecommons.org/licenses/by/4.0/>), which permits unrestricted use, distribution, and reproduction in any medium, provided you give appropriate credit to the original author(s) and the source, provide a link to the Creative Commons license, and indicate if changes were made.

References

- ASTM C1036-16.: Standard Specification for Flat Glass. ASTM Int. (2011)
- ASTM C1499-03.: Standard Test Method for Monotonic Equibiaxial Flexural Strength of Advanced Ceramics at Ambient Temperature. ASTM Int. (2009)
- ASTM G173-03.: Standard Tables for Reference Solar Spectral Irradiances?: Direct Normal and Hemispherical on 37° Tilted Surface, pp. 1–21. ASTM Int. (2012)
- BS-AU 251.: Specification for performance of automotive laminated windscreen repair systems. Br. Stand. (1994)
- Dabbs, T.P., Lawn, B.R.: Acid-enhanced crack initiation in glass. *J. Am. Ceram. Soc.* **65**(3), C37–C38 (1982)
- Datsiou, K.: Design and performance of cold bent glass. Ph.D. thesis, University of Cambridge (2017)
- Datsiou, K.C., Overend, M.: Artificial ageing of glass with sand abrasion. *Constr. Build. Mater.* **142**, 536–551 (2017a)
- Datsiou, K.C., Overend, M.: The strength of aged glass. *Glas. Struct. Eng.* **2**, 105–120 (2017b)

- Datsiou, K.C., Overend, M.: Weibull parameter estimation and goodness-of-fit for glass strength data. *Struct. Saf.* **73**, 29–41 (2018)
- Gehrke, E., Ullner, C., Hähnert, M.: Fatigue limit and crack arrest in alkali-containing silicate glasses. *J. Mater. Sci.* **26**(20), 5445–5455 (1991)
- Glass Polish Ltd.: Glass Polish: Repair, Renew Restore. <http://www.glasspolish.net> (2017). Accessed Dec 2017
- Haldimann, M., Overend, M., Luible, A.: Structural use of glass. In: International Association for Bridge and Structural Engineering. IABSE Association (2008)
- Hand, R.J., et al.: Epoxy based coatings on glass: strengthening mechanisms. *J. Non-Cryst. Solids* **315**, 276–287 (2003)
- Hayashida, K. et al.: Rationale for windshield glass system specification requirements for shuttle orbiter (1972)
- Kolli, M., et al.: HF etching effect on sandblasted soda-lime glass properties. *J. Eur. Ceram. Soc.* **29**, 2697–2704 (2009)
- MacKay, D.J.: Sustainable Energy Without the Hot Air, 1st edn. UIT Cambridge, Cambridge (2009)
- Nsg.: Pilkington and the Flat Glass Industry. *Glas. Ind.* (2010)
- Overend, M., Louter, C.: The effectiveness of resin-based repairs on the inert strength recovery of glass. *Constr. Build. Mater.* **85**, 165–174 (2015)
- Paparo, I., Overend, M.: Bending performance of glass fibre reinforced polymer sandwich panels subjected to combined thermal cycling and load, In: Proceedings of 8th International Conference on Advanced Composites Construction. Sheffield, UK, pp. 260–266 (2017)
- Schula, S.: Charakterisierung der Kratzanfälligkeit von Gläsern im Bauwesen. Ph.D. thesis, Technical University of Darmstadt (2015)
- Zaccaria, M., Overend, M.: Thermal healing of realistic flaws in glass. *J. Mater. Civ. Eng.* **4015127**, 1–9 (2015)